PAPER • OPEN ACCESS

On the transport of edge localized mode filaments in the tokamak scrape-off layer

To cite this article: J. Adamek *et al* 2020 *Nucl. Fusion* **60** 096014

OPEN ACCESS

IOP Publishing | International Atomic Energy Agency Nuclear Fusion

Nucl. Fusion **60** (2020) 096014 (5pp) https://doi.org/10.1088/1741-4326/ab9e14

On the transport of edge localized mode filaments in the tokamak scrape-off layer

J. Adamek[1], D. Tskhakaya[1], A. Devitre[2], J. Cavalier[1], J. Horacek[1], M. Komm[1], M. Sos[1,3], P. Bilkova[1], P. Böhm[1], J. Seidl[1], V. Weinzettl[1], P. Vondracek[1], T. Markovic[1], M. Hron[1], R. Panek[1], the COMPASS team[1] and the EUROfusion MST1 team[a]

[1] Institute of Plasma Physics of the CAS, Prague, Czech Republic
[2] Department of Applied Physics, Ghent University, Belgium
[3] Faculty of Nuclear Sciences and Physical Engineering, Czech Technical University, Prague, Czech Republic

E-mail: adamek@ipp.cas.cz

Received 9 April 2020, revised 1 June 2020
Accepted for publication 18 June 2020
Published 4 August 2020

Abstract

Microsecond probe measurements of the electron temperature during the tokamak edge localised mode (ELM) instability show that the peak values significantly exceed those obtained by conventional techniques. The temperatures measured at the plasma facing component (divertor) are around 80% of the initial value (at the pedestal). This challenges the current understanding, where only several percent of the pedestal value are measured at the divertor. Our results imply a negligible energy transfer from the electrons to the ions during the ELM instability, and therefore no associated increase of the ion power loads on the divertor. This observation is supported by the simple analytic free-streaming model, as well as by full kinetic simulations. The energetic ELM ion loads are expected to be one of the main divertor damaging factors; therefore, the obtained results give an optimistic prediction for next generation fusion devices.

Keywords: plasma, magnetic-confinement fusion, edge-localised mode, electron temperature, kinetic simulation

(Some figures may appear in colour only in the online journal)

1. Motivation

In order to demonstrate the viability of nuclear fusion as a source of energy, the International Tokamak Experimental Reactor (ITER) will operate in the high confinement mode (H mode) [1], for which both energy and particle confinement times are enhanced. This regime is characterized by sudden outbursts of hot and dense plasma towards the plasma-facing components (PFCs), known as edge localised modes (ELMs) [2]. The highest energy confinement time is achieved in presence of Type I ELMs [3], which are associated with undesirably high power loads to the PFCs in the most exposed area, called the divertor [4]. Previously, the power load caused by Type I ELMs was predicted for ITER [5], and other fusion devices [6, 7]. Clearly, without an efficient mitigation or suppression of ELMs, overheating of the ITER PFCs would be inevitable [8]. Even with such techniques being utilized, the occasional presence of large ELMs represents an issue with respect to the safety of the PFC. For this reason, understanding of ELM generation and its properties is essential for successful operation of future thermonuclear reactors.

An additional risk for ITER PFCs comes from material erosion, which strongly increases with the ion energy. Recent results from the Joint European Torus (JET) [9, 10] indicate that ELM ion energy at the divertor seems to be significantly higher than at the pedestal, which would enhance erosion. They consider the free-streaming kinetic model (FSM) [11, 12] in order to explain this observation. The FSM describes the propagation of initially Gaussian distributed ELM plasma particles into an empty SOL [12]. One important parameter is the ratio of the pedestal and

[a] See Labit *et al* 2019 (https://doi.org/10.1088/1741-4326/ab2211) for the EUROfusion MST1 team.

divertor temperature $\Re = T_{e,div}/T_{e,ped}$. The ratio $\Re$ is given by:

$$\frac{2}{3} < \Re = \frac{1}{3}\left(2 + \frac{1}{1+(tc_s/\lambda)^2}\right) < 1,$$

where λ represents the initial parallel elongation of ELM source, $c_s \approx \sqrt{2T_{e,ped}/m_i}$ is the ion sound speed and t is the time from the start of the ELM. In its simplest form, the FSM predicts $2/3 < \Re < 1$. However, the JET results [9, 10], obtained by conditionally-averaged (CAV) the signal of several swept Langmuir probes, yield $\Re = T_{e,div}/T_{e,ped} \ll 1$. They have suggested that this discrepancy between experimental observations and the FSM could be explained by the role of Coulomb collisions within ELM filaments, enabling a transfer of energy between the electrons and the ions. Consequently, the ELM ion energy would significantly exceed the pedestal value. However, it remains unclear whether the specific plasma conditions inside filaments are indeed responsible for such dramatic modification of $\Re$ and ion energy.

For COMPASS [13] parameters, $\lambda < 1$ m and $T_{e,ped} \sim 300$ eV, already in ~ 10 μs $\Re$ will drop to 2/3. Fast measurements ($\ll 10$ μs) are therefore required for a quantitative study of this process. The aim of this work was to perform dedicated fast measurements of the divertor electron temperature during the ELMs [13], to calculate the corresponding ratio $\Re$ and to compare it with FSM predictions and full kinetic simulations of ELM propagation in the scrape-off layer (SOL).

2. Experiment—ratio of elm and pedestal electron temperature

Previous experiments on COMPASS, ASDEX Upgrade, MAST and ISTTOK [14–17] tokamaks have shown that the combination of a ball-pen probe (BPP) and a Langmuir probe (LP) can provide the value of the electron temperature using the floating BPP (Φ^{BPP}) and LP (V_{fl}^{LP}) potentials and the formula $T_e = (\Phi^{BPP} - V_{fl}^{LP})/\alpha$. The coefficient α is given by the characteristics of the LP and the BPP, $\alpha = \alpha^{LP} - \alpha^{BPP}$, as it is discussed in [7, 14, 15]. Our investigation of the ELM electron temperature on the COMPASS divertor is performed with a high temporal resolution (in the order of 1 μs) within the range ($T_{e,div} < 400$ eV), using a recently built system of BPPs and roof-top shaped LPs with the coefficient $\alpha = 1.4$ [7]. These parameters are sufficient to resolve the filamentary structure of an ELM. The neighboring BPP and LP probes are toroidally separated only by ~ 2 cm, which ensures nearly local measurements (corresponding to ~ 0.5 mm cross-field distance $\ll$ typical filament size) of the electron temperature on divertor. Note that the characteristics of BPP and LP were investigated during L-mode discharges [7] and cannot be directly obtained within the ELM events. Therefore, the coefficient α^{LP} of the LP during ELM might be affected by different value of the ratio of the ion to electron temperature. However, the value of α^{LP} is proportional to the logarithm of the ion sound speed, which is proportional to the square root of the temperature ratio. The resulting α^{LP} is weakly dependent on this ratio. We have also observed on COMPASS (figure 3 and figure 4 in [18]) and ASDEX Upgrade (figure 4 in [19]) that BPP can sustain its characteristics during ELMs. It is worth mentioning that the ELM energy fluence ($\varepsilon_{||} = \int \gamma T_e j_{sat} dt$, with $\gamma = 7$ for the heat transmission coefficient) using fast ELM electron temperature measurements as well as the ion saturation current density (j_{sat}) are in good agreement with Eich's model prediction [5, 7] and with infrared camera measurements (figure 8.20 in [20]).

For each ELM, we report the peak value of the electron temperature at different radial position on the outboard divertor; see e.g. figure 1. This profile was then fitted using the function (equation 2) in [21], to obtain a representative maximum, $T_{e,div,max}$, with an estimate of its error bar. The fitting function was adapted for T_e by removing the background value and it clearly follows the majority of our achieved profiles.

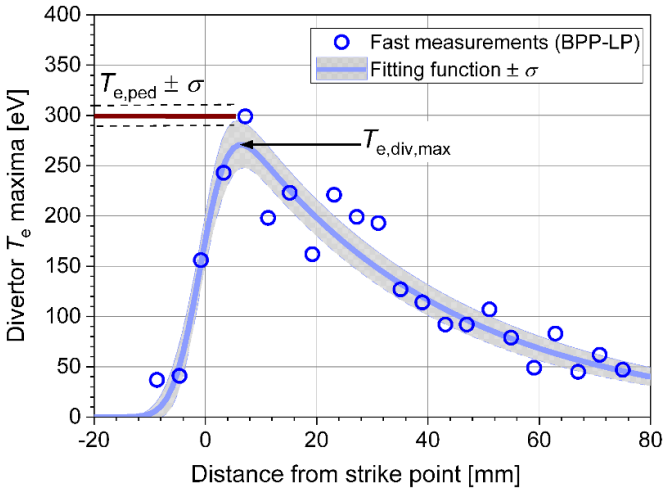

Figure 1. Example of an outboard radial profile of T_e peak (maxima) values obtained during a single ELM event (NBI assisted H-mode #18235) using fast measurements (BPP-LP). The profile is fitted by the function (equation 2) in [21] with no background value.

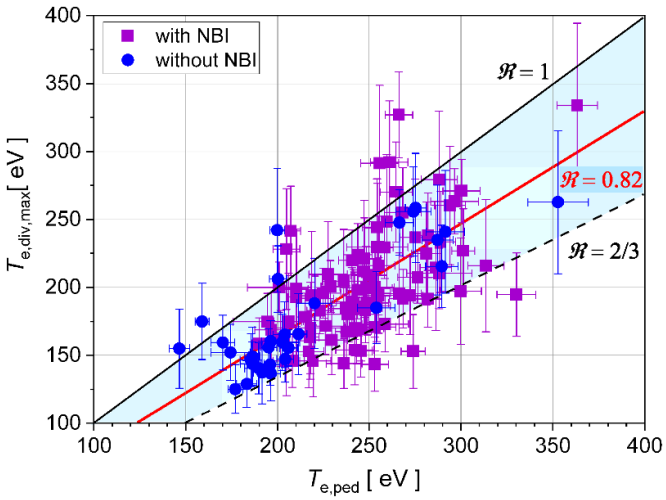

Figure 2. Comparison of the ELM electron temperature maximum on the divertor to the corresponding pedestal temperature in 125 ELM events with a final averaged ratio $\Re = 0.82$. The black lines show the maximum and minimum values predicted by the FSM.

The divertor probe measurements are compared to the pedestal electron temperature, $T_{e,ped}$, obtained by a high-resolution Thomson scattering system [22] in the last 30% of the previous ELM cycle (corresponding to fully developed H-mode pedestal). The value $T_{e,ped}$ is then determined by the two-line technique [23]. The experimental value of the ratio between divertor and pedestal electron temperature is then calculated as $\Re = T_{e,div,max}/T_{e,ped}$. In the particular case of the ELM plotted in figure 1, $T_{e,div,max} = 271 \pm 23$ eV, $T_{e,ped} = 300 \pm 10$ eV leading to $\Re = 0.90 \pm 0.08$. This example shows that the maximum of the ELM electron temperature on the divertor, coming from one filament, can be close to the pedestal temperature, indicating that there is no transfer of electron energy to the ions, and no interaction with the pre-ELM divertor plasma. We have analyzed 45 ELMy H-mode discharges with plasma parameters ranging from $1.1 < B_T$ [T] < 1.4; $220 < I_P$ [kA] < 300; $2.5 < n_e$ [10^{19} m^{-3}] < 10; with and without NBI heating. This yielded 125 ELM events in which Thomson scattering flashed in the pre-ELM period with fully developed H-mode pedestal. The resulting values of $T_{e,div,max}$ were obtained for pedestal temperatures within the range of $180 < T_{e,ped}$ [eV] < 350, as shown in figure 2. This interval represents almost the full range of the pedestal temperatures, which we are capable to achieve on COMPASS. Most points are found to be with ratio $\Re$ below 1 and within the boundaries of the FSM (light blue area with black lines). The ratio $\Re$ has no clear dependence on the line averaged density n_e (see figure 3), the toroidal magnetic field B_T or the plasma current I_p. The relative ELM energy $\Delta W/W$ (W is the total pre-ELM plasma energy) varied within the wide range of $2\% < \Delta W/W < 10\%$, with obviously no influence on $\Re$; see figure 4. An average value was therefore calculated using all ELM events as $\Re = 0.82 \pm 0.13$, which fits the FSM prediction of $2/3 < \Re < 1.0$ (section 1) within the statistical range. In addition, the maxima of the conditionally-averaged (CAV) ELM electron temperature were compared to the pedestal electron temperatures in order to investigate the influence of the CAV technique. The CAV [24] ELM were obtained from fast (BPP-LP) electron temperature measurements by averaging a set of similar ELMs synchronized by the marker (here we use D_α signal) as it was shown in our previous work for upstream and divertor measurements (figure 7 and figure 9 in [18]). Then, we obtain CAV ELM electron temperature for each BPPs-LPs and we take the maximum value of the electron temperature and its error bar on the divertor. The CAV technique will cause a smoothing of the filamentary structure of the ELMs and their peak values due to the irregular structure (different temporal evolution and amplitude) of the filaments within each single ELM event, as it can be seen in [18] We note it is even more tricky to reconstruct LP I–V characteristic during ELMs in order to obtain the CAV ELM electron temperature as it is used in JET divertor [9, 10]. Nineteen different ELM series consisting of well reproduced ELMs and stationary plasma conditions—produced a ratio $\Re_{CAV} = 0.58 \pm 0.11$, smaller than the one obtained from the peak values ($\Re = 0.82 \pm 0.13$). As expected, the CAV technique underestimates the resulting divertor ELM electron temperature due to randomly averaging filaments of each ELM. However, both values are still much higher than those obtained on JET [9] and close to the prediction of FSM for vacuum, disregarding electron-electron Coulomb collisions.

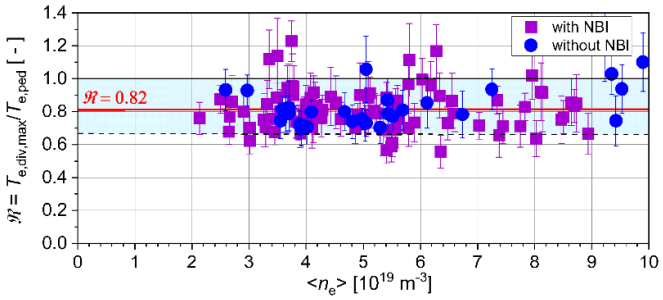

Figure 3. The ratio $\Re$ versus the line averaged density n_e for ELMs with and without NBI heating. The black lines show the maximum and minimum values predicted by the FSM.

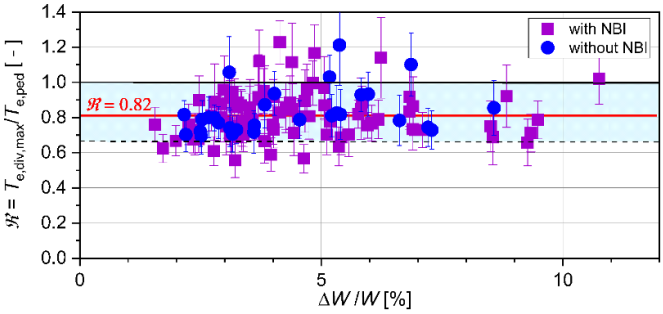

Figure 4. The ratio $\Re$ versus the relative ELM energy $\Delta W/W$ with and without NBI heating. The black lines show the maximum and minimum values predicted by the FSM.

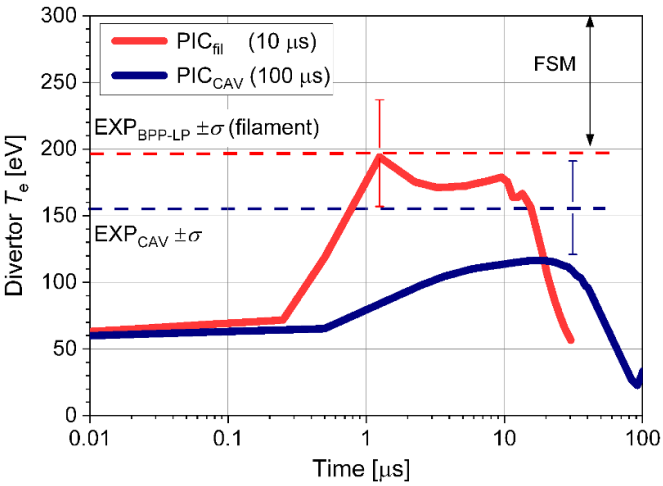

Figure 5. Temporal evolution of the ELM electron temperature on the outboard divertor obtained from PIC simulation for $Te,ped = 300$ eV for a single filament (PIC_{fil}, 10 μs) and the corresponding CAV ELM (PIC_{CAV}, 100 μs). The experimental value of divertor $T_{e,max}$ obtained from fast single ELM measurements (EXP_{BPP-LP}) and the CAV (EXP_{CAV}) technique (for 9 reproducible ELMs with averaged $T_{e,ped} = 306 \pm 10$ eV) in shot #18463 as well as the limit of the FSM are shown for comparison.

3. Comparison—1D kinetic simulations

To better interpret the experimental results, we performed 1D3V (1-dimensional in usual and three-dimensional in velocity spaces) kinetic simulations of ELM propagation through the SOL, using the electrostatic particle-in cell Monte Carlo code BIT1. The simulation geometry is a one-dimensional flux tube adjacent to the separatrix and bounded by the inner and outer divertor plates [25]. The particle and heat source implemented at the outer midplane (OMP) mimics a cross-field transport through the separatrix. Simulations include electrons, D^+ ions, D atoms and impurity particles, C and C^+. Carbon atoms originate from physical sputtering at the divertor surfaces. Complete set of elastic (including Coulomb collisions) and inelastic collisions between simulated particles is included in the model; details are provided in [25, 26]. For simplicity we use a reduced model of plasma recycling: ions absorbed at the divertor plates are recycled as atoms and we do not include higher ionization states $C^{+i>1}$. The simulation consists of three phases corresponding to the inter-ELM, ELM-ing and after-ELM SOLs. The ELM event is simulated by instantaneous increase of particle source intensity and temperature, corresponding to the ELM reconnection. This model shows good agreement with experimental observations [27]. The connection length (15 m from inner to outer divertor), the average strength of the magnetic field (1 T) and the inclination angle of the magnetic field with respect to the divertor plates (1.5°) were taken from the equilibrium reconstruction code EFIT. These values are fixed for all three phases. Simulation parameters for the inter-ELM phase were adjusted to obtain typical ELMy H-mode parameters at the OMP and the divertor, $n_{\mathrm{omp}} \sim 10^{19}$ m^{-3} and $T_{\mathrm{e,omp}} \sim 60$ eV measured by Thomson scattering diagnostic. The ELM phase was simulated by increasing the intensity and temperature of the particle source at the OMP, $T_{\mathrm{ELM}} = T_{\mathrm{ped}} = 300$ eV. The intensity of the ELM particle source corresponds to the upper limit in ELM size, estimated from Eich's model [5], on the outboard divertor $\varepsilon_{\parallel} = 75$ kJ m^{-2} [7] (for the nearest experimental ELM parameters in discharge #18463: $T_{\mathrm{e,ped}} = 300 \pm 11$ eV, $B_{\mathrm{T}} = 1.12$ T). Two cases were considered for ELM duration: 10 μs and 100 μs. The former value 10 μs was used to model the filamentary structure of the ELM and corresponds to the time of arrival of the first filament. To simulate the effect of one dominant filament we assume that this first filament carries half of the ELM energy. The latter corresponds to the lower limit of ELM reconnection time during the discharge and was used to mimic an averaged ELM (no filament), comparable to the CAV ELM technique. The after-ELM phase was simulated by reducing the particle and heat sources to the inter-ELM values.

In order to ensure high resolution, in average 10^4 particles were used in each cell (the simulation required ~ 10^6 CPU hours). The figure 5 shows a simulated temporal evolution of the ELM electron temperature ($\mathrm{PIC_{fil}}$ for 10 μs and $\mathrm{PIC_{CAV}}$ for 100 μs) at the outboard divertor with resulting $T_{\mathrm{e,div,max}}$ (fil) = 195 eV and $T_{\mathrm{e,div,max}}$ (CAV) = 116 eV, which yields $\Re_{\mathrm{fil}} = 0.65$ and $\Re_{\mathrm{CAV}} = 0.39$. The PIC simulation ($\mathrm{PIC_{fil}}$—10 μs) results are in a good agreement with experimental value obtained from fast (BPP-LP) measurements of a single ELM in discharge #18463. However, the PIC simulation with 100 μs ELM duration provides significantly lower divertor temperature then in the previous case. Although, the $T_{\mathrm{e,div,max}}$(CAV) is below the experimental value of the CAV ELM value, it confirms that neglecting the filamentary structure of the ELM leads to an under estimations of divertor temperature maximum. It is seen in the figure 5 that there is an agreement within the experimental error bars which we classify as a quantitatively very good agreement with the simplified 1D model.

4. Conclusion

Microsecond measurements of the divertor electron temperature have been performed on COMPASS for 125 ELM events in 45 ELMy H-mode discharges. The peak values were compared to the corresponding pedestal temperature. The resulting averaged ratio $\Re = 0.82 \pm 0.13$ fits the prediction of the free-streaming model $2/3 < \Re < 1.0$. On the other hand, the ratio obtained from conditionally-averaged ELMs is lower, $\Re_{\mathrm{CAV}} = 0.58 \pm 0.11$, as expected due to the averaging of the filaments. Both values are much higher than those obtained on JET ($\Re_{\mathrm{CAV}} \lesssim 0.05$) showing no influence of Coulomb collisions, which were deemed responsible for the transfer of energy from electrons to ions in [9]. The ratio obtained from 1D kinetic simulations of fast 'filament-resolved' and slow 'conditionally averaged' ELMs supports our experimental findings. Good agreement between the free-streaming model, kinetic simulations and the experiments is connected to the low collisionality of the outer SOL in COMPASS, where inelastic processes are negligible during the ELM. In summary, ELM filament-resolved electron temperature measurements on COMPASS point to: (i) a low energy transfer from electrons to ions. This leads to a lower physical sputtering of material of the divertor PFC; and (ii) a significant underestimation of the the maximum values of the divertor ELM electron temperature by the conditionally-averaged technique.

Acknowledgments

The first author would like to thank R. Pitts for the initial discussion on the free-streaming model. This work has been carried out within the framework of the EUROFusion Consortium and has received funding from the Euratom research and training programme 2014–2018 and 2019–2020 under Grant Agreement No. 633053. The views and opinions expressed herein do not necessarily reflect those of the European Commission. It was supported by MYES projects # LM2015045 and CZ.02.1.01/0.0/0.0/16_013/0001551 and IAEA CRP F13019—Research Contract No. 22727/R0. The 1D kinetic simulations were performed on the Marconi supercomputer. This work was also supported by the Czech Science Foundation within the project GACR 20-28161S (PIC simulation results) and GA19-15229S (Thomson scattering data analysis).

ORCID iDs

J. Adamek https://orcid.org/0000-0001-8562-1233
A. Devitre https://orcid.org/0000-0001-7428-0373
J. Horacek https://orcid.org/0000-0002-4276-3124
J. Seidl https://orcid.org/0000-0002-8675-8431
V. Weinzettl https://orcid.org/0000-0001-8936-7578

References

[1] ITER Physics Expert Group on Confinement and Transport *et al* 1999 *Nucl. Fusion* **39** 2175
[2] Ongena J., Koch R., Wolf R. and Zohm H. 2016 *Nat. Phys.* **12** 398–410
[3] Eich T. *et al* 2005 *Plasma Phys. Control. Fusion* **47** 815–42
[4] Pitts R.A. *et al* 2019 *Nucl. Mater. Energy* **20** 100696
[5] Eich T., Sieglin B., Thornton A.J., Faitsch M., Kirk A., Herrmann A. and Suttrop W. 2017 *Nucl. Mater. Energy* **12** 84–90
[6] Eich T., Herrmann A. and Neuhauser J. 2003 *Phys. Rev. Lett.* **91** 195003
[7] Adamek J. *et al* 2017 *Nucl. Fusion* **57** 116017
[8] Gunn J.P. *et al* 2017 *Nucl. Fusion* **57** 046025
[9] Guillemaut C., Metzger C., Moulton D., Heinola K., O'Mullane M., Balboa I., Boom J., Matthews G.F., Silburn S. and Solano E.R. 2018 *Nucl. Fusion* **58** 066006
[10] Guillemaut C. *et al* 2015 *Plasma Phys. Control. Fusion* **57** 085006
[11] Fundamenski W. and Pitts R.A. 2006 *Plasma Phys. Control. Fusion* **48** 109–56
[12] Moulton D., Ghendrih P., Fundamenski W., Manfredi G. and Tskhakaya D. 2013 *Plasma Phys. Control. Fusion* **55** 085003
[13] Panek R. *et al* 2016 *Plasma Phys. Control. Fusion* **58** 014015
[14] Adamek J. *et al* 2016 *Rev. Sci. Instrum.* **87** 043510
[15] Walkden N.R., Adamek J., Allan S., Dudson B.D., Elmore S., Fishpool G., Harrison J., Kirk A. and Komm M. 2015 *Rev. Sci. Instrum.* **86** 023510
[16] Silva C., Adamek J., Fernandes H. and Figueiredo H. 2015 *Plasma Phys. Control. Fusion* **57** 025003
[17] Horacek J., Adamek J., Müller H.W., Seidl J., Nielsen A.H., Rohde V., Mehlmann F., Ionita C. and Havlíčková E. 2010 *Nucl. Fusion* **50** 105001
[18] Adamek J. *et al* 2017 *Nucl. Fusion* **57** 022010
[19] Adamek J. *et al* 2010 *Contrib. Plasma Phys.* **50** 854–9
[20] Vondracek P. 2019 *Plasma Heat Flux to Solid Structures in Tokamaks* Phd thesis (Charles University, Czech Republic) Doctoral Thesis Plasma Heat Flux to Solid Structures in Tokamaks (https://is.cuni.cz/webapps/zzp/detail/123000/?lang=en)
[21] Eich T., Sieglin B., Scarabosio A., Fundamenski W., Goldston R.J. and Herrmann A. 2011 *Phys. Rev. Lett.* **107** 215001
[22] Bilkova P., Bohm P., Aftanas M., Sos M., Havranek A., Sestak D., Weinzettl V., Hron M. and Panek R. 2018 *J. Instrum.* **13** C01024
[23] Schneider P.A. *et al* 2012 *Plasma Phys. Control. Fusion* **54** 105009
[24] Pitts R.A. 2003 *Nucl. Fusion* **43** 1145–66
[25] Tskhakaya D. 2017 *Plasma Phys. Control. Fusion* **59** 114001
[26] Tskhakaya D., Jachmich S., Eich T. and Fundamenski W. JET EFDA Contributors 2011 *J. Nucl. Mater.* **415** S860–S864
[27] Tskhakaya D., Pitts R.A., Fundamenski W., Eich T., Kuhn S. JET EFDA Contributors 2009 *J. Nucl. Mater.* **390–391** 335